SAXS Study of Formation and Growth of Tin Oxide Nanoparticles in the Presence of Complexing Ligands

L. Broussous,[†,‡] C. V. Santilli,[*,‡] S. H. Pulcinelli,[‡] and A. F. Craievich[§]

Laboratoire des Matériaux et Procédés Membranaires, ENSCM, 34 296 Montpellier, France, Instituto de Química, UNESP, P.O. Box 355, 14800-900, Araraquara, SP, Brazil, and Instituto de Física, USP, P.O. Box 66318, 05315-970, São Paulo, SP, Brazil

Received: July 13, 2001; In Final Form: November 1, 2001

The effect of acetylacetone (acac) complexing ligand on the formation and growth of tin oxide-based nanoparticles during thermohydrolysis at 70 °C of a tin precursor $SnCl_{4-n}(acac)_n$ ($0 \leq n \leq 2$) solution was analyzed by in situ small-angle X-ray scattering. A transparent and stable sol was obtained after 2 h of thermohydrolysis at 70 °C, allowing the quantitative determination of the particle volume distribution function and its variation with the reaction time. The number of colloidal particles for equivalent thermohydrolysis temperature and time decreases as the [acac]/[Sn] ratio in initial solution increases from 0.5 to 6. Instead, the amount of soluble species remaining in solution increases for increasing [acac]/[Sn] ratio within the same range. This indicates that increasing amounts of Sn−acetylacetone complexes partially prevent the hydrolysis and consequent formation of colloidal particles. The N_2 adsorption isotherm characterization of freeze-dried powders demonstrates that the average pore size is approximately equal to the average size (≈9 Å) of the colloidal primary particles in the sol, and that the porosity and surface area (≈200 $m^2\ g^{-1}$) are independent of the acac content in the initial solution.

1. Introduction

Thin films composed of SnO_2 nanoparticles obtained by the sol−gel procedure have promising applications as nanofiltration membranes,[1] transparent electrodes,[2] and anticorrosion coatings.[3] The improvement of electrical conductivity and anticorrosion properties of this type of material requires high-density thin films that are difficult to achieve at low sintering temperatures.[4] The sol−gel procedure offers an alternative path for tailoring the porosity and for controlling the nanotexture of the derived film.[5]

The possibility of structure control at a molecular level by sol−gel chemistry has been demonstrated for silica and silicate derivative materials. For these systems, the correlation between the structure of the precursor sols and the nanostructural features (pore size, surface area, sintering characteristics) of the derivative powders and coatings has been established.[5] Unfortunately, tin precursors, like other metals of interest to ceramists (Ti, Zr, Al), have rates of hydrolysis and condensation a few orders of magnitude higher than for Si, leading to a quick precipitation of tin oxo-compounds.

Livage et al.[6] have attempted to reduce the homogeneous crystal growth and final size in ceramic powders by varying the conditions of hydrolysis and condensation of transition metal−alkoxide compounds. They emphasized that oligomerization, solvent modification, variation in acid/base catalysis condition, and/or chemical modification of the precursors by the addition of complexing ligands may be used to try to slow condensation. The substitution of easily hydrolyzable groups in the metal coordination sphere by weakly hydrolyzable complexing ligands, such as β-diketones, lowers the functionality of the precursor, thus decreasing their reactivity toward hydrolysis−condensation.[7−11] Moreover, the driving force of reactivity of similar tetravalent metal precursors ($Ti(OR)_4$, $Sn(OR)_4$) toward the nucleophilic species is related to the possibility of the metallic center expanding its coordination. Complexed precursors that can easily reach a 6-fold coodination exhibit a lower hydrolytic reactivity.[7,8] Complexing ligands may also act as surface protecting agents, increasing the stability of the colloidal particles and improving the property of powder redispersibility.[10,11]

In the specific case of SnO_2-based materials, we have recently demonstrated[12] that nanoparticles prepared by thermohydrolysis in ethanol have nanostructural features similar to those obtained by alkaline hydrolyses of $SnCl_4$ aqueous solutions.[13] Furthermore, the resulting freeze-dried powders are fully redispersible in water or in alcohol without any surface additive. An important aspect of the ethanolic route is the relatively low porosity in the derived coating films, about 28%, as compared with the value of 52% observed for coatings prepared from aqueous solutions. This different behavior was attributed to the precipitation of unhydrolyzed species inside the pores during the drying process.[12] This also suggests that the porosity of SnO_2 films can be tailored by controlling the relative amount of unhydrolyzed precursor in the sol.

In this paper we study the effect of acetylacetone (acac) on the hydrolysis reaction and the nanostructural features of SnO_2 colloidal particles obtained by thermohydrolysis of the precursor ethanolic solution. The effects of the nominal complexing ratio, c =[acac]/[Sn], on the kinetics of colloidal particle formation were analyzed by small-angle X-ray scattering (SAXS). The experiments were performed in situ during the thermohydrolysis process.

* Author to whom correspondence should be addressed.
† Laboratoire des Matériaux et Procédés Membranaires, ENSCM.
‡ Instituto de Química, UNESP.
§ Instituto de Física, USP.

10.1021/jp012700b CCC: $22.00
Published on Web 02/26/2002

2. Experimental Section

2.1. Sample Preparation. The precursor solution was prepared by dissolving 0.09 mol/L of tin tetrachloride in ethanol. Different amounts of acetylacetone were added at room temperature to the solution to yield [acac]/[Sn] nominal complexing ratios of 0, 0.5, 1.0, 2.0, and 6.0. They are referred to as Ac0, Ac05, Ac1, Ac2, and Ac6, respectively. Water was added to the solution to yield a hydrolysis ratio $[H_2O]/[Sn] = 100$. The acid (pH $\cong$ 1) solutions were put into closed cells and the thermohydrolysis was carried out at 70.0 $\pm$ 0.5 °C, giving rise to transparent and stables sols. No precipitation was observed during the first 2 h of thermohydrolysis. After 65 min at 70 °C, the suspensions were cooled to room temperature. Aliquots of 15 mL of so-prepared suspensions were put inside acetylcellulose membranes tubing (12−14000 MW) and then submitted to static dialysis against 100 mL of aqueous ammonium solution (pH = 9) to eliminate as much as possible unhydrolyzed cations and other soluble species. The aqueous ammonium solution was changed each 8 h for 6 days. Irrespective of the [acac]/[Sn] ratio, a transparent gel was formed as the pH of the suspension reaches values about 4−5, corresponding to the isoelectric point of SnO_2.[1] The increase of pH to 7 with the elapse of dialysis leads to repeptization and formation of transparent and kinetically stable colloidal suspensions. No precipitation was observed during dialysis of samples prepared with $c \leq 2$, while for $c = 6$ the precipitation of an amorphous acetylacetone derivative was observed. After separation of the precipitate by filtration, the colloidal particles were isolated from suspension by freeze-drying at −5 °C and pressure of ~1 μmHg. The gravimetric analyses of the powdered samples indicate that almost 70% of the tin atoms are lost during the dialysis of samples prepared with $c \leq 2$, while 95% are in the precipitate isolated by filtration of Ac6.

2.2. Sample Characterization. The structural features of the colloidal suspensions formed during thermohydrolysis were studied by SAXS. The measurements were performed in situ using the SAS beamline at the Brazilian National Synchrotron Light Laboratory (LNLS). This beamline is equipped with an asymmetrically cut and bent silicon (111) monochromator yielding a monochromatic (λ = 1.608 Å) and horizontally focused beam.[14] Because of the small size of the incident beam cross-section at the detection plane, no mathematical desmearing of the experimental SAXS function was needed. A gas position-sensitive X-ray linear detector and a multichannel analyzer were used to record the SAXS intensity, $I(q)$, as a function of the modulus of the scattering vector $q = (4\pi/\lambda) \sin \theta$, θ being half of the scattering angle. The parasitic X-ray scattering from slits and air was subtracted from the total scattering intensity. The resulting curves were corrected for effects of variations in the linear detector sensibility along its window. To be able to compare the intensity produced by each sample during hydrolysis, the scattering intensities were normalized to account for the natural decay in intensity of the synchrotron source. To make possible a comparison between different samples the intensities were also multiplied by sample attenuation and normalized to equivalent sample thickness. The SAXS data collection started just after placing the sample into closed cells maintained at a constant temperature (T = 70 °C). Each spectrum was collected during a time interval of 150 s.

The texture of freeze-dried powders was analyzed by nitrogen adsorption isotherm (77 K) measurements. Data collection was performed by the static volumetric method, using an ASAP2010 (Micromeritics) instrument equipped with an extra molecular drag pump. Before each measurement, the samples were degassed at 100 °C by vacuum pumping for a time interval high enough to attain a constant pressure (~1 μmHg).

2.3. SAXS Method. To analyze the SAXS data it was assumed that the scattering is produced by a system consisting of a polydisperse set of SnO_2-based colloidal particles of nearly spherical shape embedded in a homogeneous (liquid) matrix. Due to the low amount of particles in suspension (<0.06 V%), it was also assumed that interference effects of the scattering amplitude produced by the different SnO_2 colloidal particles are negligible. We have considered that this system can be approximately described by a two-electron density model.[15] One of the phases corresponds to the SnO_2 colloidal particles and the other to the liquid solvent containing a fraction of remnant-soluble precursor.

The asymptotic behavior, at high q, of the SAXS intensity, $I(q)$, produced by an isotropic two-electron density structure is given by Porod's law:[15]

$$I(q) = 2\pi \, \Delta\rho^2 \, S/q^4 \tag{1}$$

where $\Delta\rho$ is the difference in electron density between the colloidal particles and the solvent, and S is the interface area. Electronic density fluctuations in both phases yield a constant contribution B to SAXS intensity, so that

$$I(q) = A/q^4 + B \tag{2}$$

where $A = 2\pi \, \Delta\rho^2 \, S$. We have assumed that the main contribution to SAXS intensity due to electron density fluctuations is produced by isolated species of soluble precursor embedded in the solvent. Under this assumption, B is proportional to the number of isolated precursor molecules remaining in solution.

The first step in data analysis focused on the asymptotic part of the experimental SAXS intensity, at large q. We determined the constant contribution B using Iq^4 versus q^4 plots and subtracted it from the total scattering intensity ($I_e(q)$), $I(q) = I_e(q) - B$. By applying the GNOM program[16] to the resulting $I(q)$ function, we determined the particle volume distributions, $V(R)$, corresponding to the different studied sols. The density particle number $N(R)$ and the total particle number N were calculated from the volume distribution $V(R)$ by applying

$$N(R) = \frac{3 \, V(R)}{4\pi \, R^3} \tag{3}$$

$$N = \int_0^\infty N(R) \, \mathrm{d}R \tag{4}$$

where R is the radius of particles.

3. Results and Discussion

3.1. Nanostructural Evolution during Thermohydrolysis. Sets of SAXS curves were measured in situ during thermohydrolysis at 70 °C for Ac0, Ac05, Ac1, Ac2, and Ac6 samples. The curves corresponding to Ac0, Ac05, and Ac6 are plotted in Figure 1. For Ac0 sample, without acetylacetone addition, the SAXS curves are nearly time invariant and indicate the presence, from the beginning, of colloidal particles. This confirms the fact that the hydrolysis and condensation processes are very fast in solutions without acetylacetone addition and indicates that the SnO_2-based colloidal particles reach their equilibrium configuration before starting the thermohydrolysis process at 70 °C.

On the contrary, the intensity of SAXS curves corresponding to all samples to which acetylacetone was added exhibit a clear

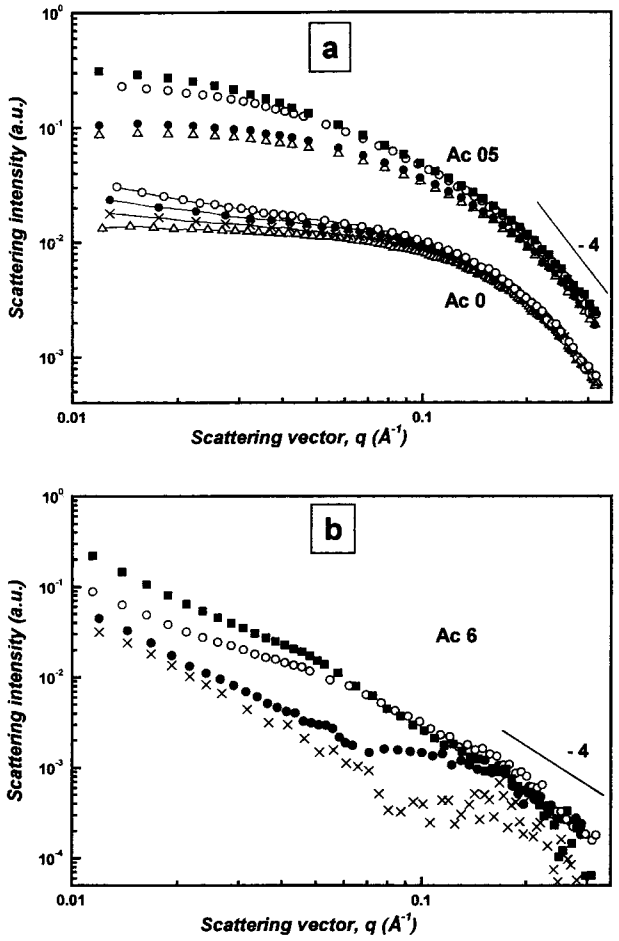

Figure 1. SAXS intensity along thermohydrolysis at 70 °C corresponding to samples (a) Ac0, Ac05, and (b) Ac6. Key to symbols corresponding to the hydrolysis time: (Δ) 5 min, (x) 15 min, (●) 30 min, (○) 65 min, and (■) 100 min. The scale factor is the same for all curves belonging to each acetylacetone content. The sets of curves corresponding to each acetylacetone content are vertically displaced for clarity.

growth during thermohydrolysis at 70 °C, as can be seen in Figures 1a and 1b for Ac05 and Ac6 samples, respectively. For an Ac05 sample, all SAXS curves for increasing hydrolysis time approximately overlap in the Porod region (high q-range) and the scattered intensity at lower q-range increases with the reaction time. The slope of the curves at small q increases with time of hydrolysis, indicating the progressive growth of the colloidal particles. Ac1 and Ac2 samples have a time evolution similar to that observed for Ac05. The features of SAXS curves corresponding to Ac6 samples exhibit a qualitatively different behavior (Figure 1b), suggesting a more complex process of particle growth.

The particle volume distributions of Ac0, Ac05, Ac1, Ac2, and Ac6 sols for different thermohydrolysis time intervals were determined using the GNOM package.[16] The results corresponding to Ac0, Ac05, and Ac6 are plotted in Figure 2. Different trends are observed, depending on acetylacetone content. In the sol without acetylacetone, the particle volume distribution function is independent of the thermohydrolysis time. On the contrary, in sols containing acetylacetone as a complexing agent, the integral of the volume size distribution starts from a relatively low value and progressively increases with reaction time. Except for Ac05, its value after 1 h of thermohydrolysis remains lower than for the acetylacetone-free sol (Ac0). For high acetylacetone content (Ac6) an important broadening of the volume distribution function occurs, indicating that the colloidal particles partially aggregate. The average particle radii are nearly time invariant for $0 < c < 2$, while a clear particle size growth is verified for $c \geq 2$.

The total number of particles as a function of the reaction time is shown in Figure 3. We note that, in the sample without acetylacetonate, almost all of the colloidal particles are formed during the heating process and are present from the beginning of the isothermal thermohydrolysis process. We also remark that the number of particles for $t = 0$ (i.e., formed before the isothermal hydrolysis) is progressively lowered by increasing additions of acetylacetone. This makes evident that acetylacetonate slows down the process of formation of colloidal particles. On the other hand, the relatively large number of particles observed at the initial time period, as compared with the number at the end of hydrolysis, indicates that a fraction of particles nucleate and grow to a kinetically stable size during the heating to 70 °C. This feature is a consequence of the low reactivity of acetylacetone ligand and of the hydrolysis ratio ($h = 100$), that lead to prompt hydrolysis of the Sn−Cl groups. During the isothermal period of thermohydrolysis, the samples containing $0 < c < 2$ have a more pronounced increase in the number of particles, while the average particle radius stays invariant. This suggests that the reactivity of the complexing ligand toward the hydrolysis−condensation is more important, which may have its reason in hindered keto−enol equilibrium due to the low amount of free acetylacetone in solution. Furthermore, as discussed in the next section, the formation of the unstable dimeric mono-chelate complex may contribute to this reactivity.

The broadening of particles size distribution with the increase in reaction time, without a major increase in particle number, indicates that the presence of an excess of acetylacetone (Ac6 sample) favors either the growth or the aggregation of particles initially formed. This effect may be associated with electrostatic destabilization of the suspension due to the high ionic strength of this solution that contains a considerable amount of unreacted soluble precursor.

3.2. Effect of Complexing Ratio. Double logarithmic plots of the scattered intensity, $I(q) = I_e(q) - B$ and $I_e(q)$, versus the modulus of the scattering vector, q, corresponding to the five studied sols after 65 min of thermohydrolysis treatment at 70 °C are shown in Figure 4. The scattered intensity of unheated samples is low and practically independent of q, typical of homogeneous solution of small molecules.

In the high q range, all log $I_e(q)$ versus log q curves (dashed line) corresponding to samples treated at 70 °C have a slope higher than −4. This suggests that a nonnegligible contribution to SAXS intensity comes from electronic density fluctuations. Iq^4 versus q^4 plots of the scattering intensity exhibit a linear dependence at high q indicating that eq 2 applies. The constant contribution from soluble species to the scattering intensity, B, was determined as the slope in the linear range of Iq^4 versus q^4 plots and then subtracted from experimental intensity $I(q) = I_e(q) - B$.

By applying the GNOM package[16] to the $I(q)$ functions, the particle volume distribution functions, $V(R)$, were determined and plotted in Figure 5. The good agreement observed in Figure 4 between the experimental $I(q)$ curves and the calculated ones from the $V(R)$ functions (continuous line), indicates that the model we have assumed is acceptable, i.e., the scattering objects can be described as a dilute set of homogeneous spherical particles.

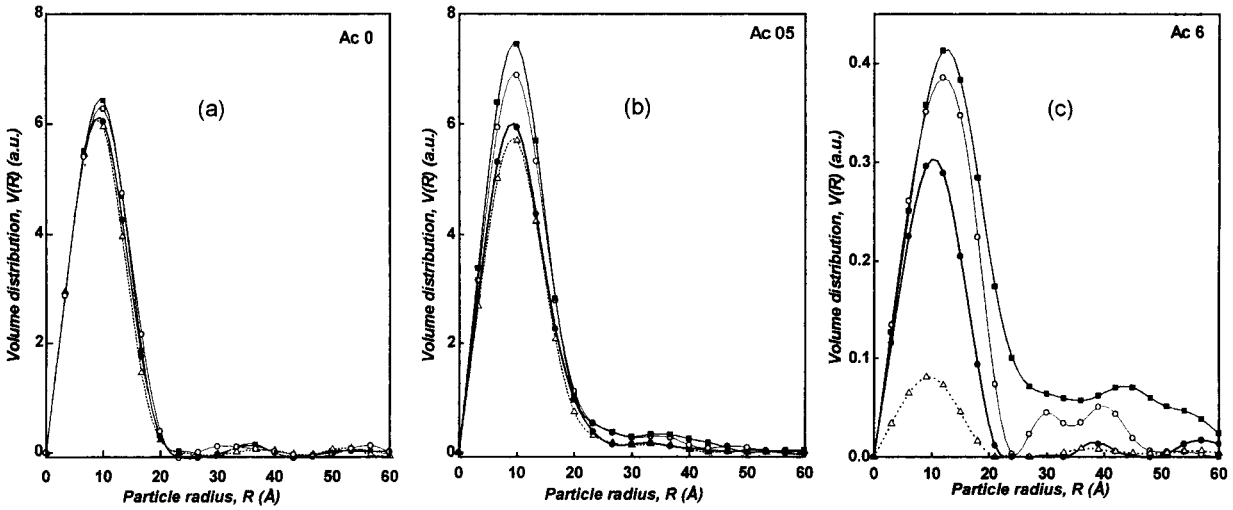

Figure 2. Volume distribution function of the colloidal particles corresponding to sols prepared with different complexing ratio (Ac0, Ac05, and Ac6) for different times of isothermal hydrolysis at 70 °C. Key to symbols corresponding to the hydrolysis time: (- -Δ- -) 5 min, (—●—) 30 min, (—○—) 65 min, and (—■—) 100 min. All curves have the same scale factor.

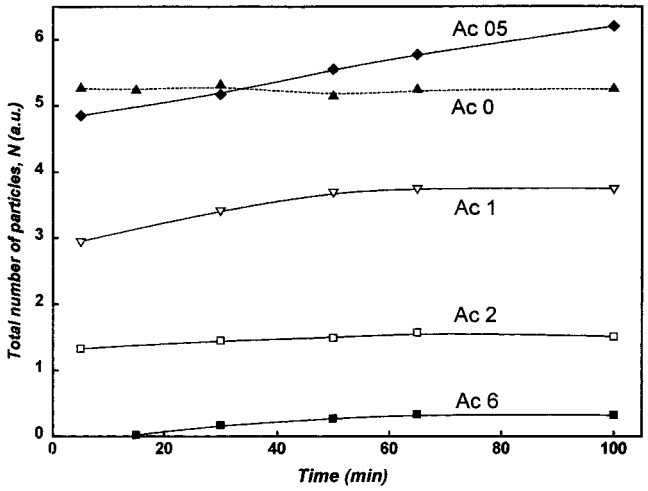

Figure 3. Total number of colloidal particles as a function of the time of hydrolysis for a sol without acetylacetone (dashed line) and with different acetylacetone contents.

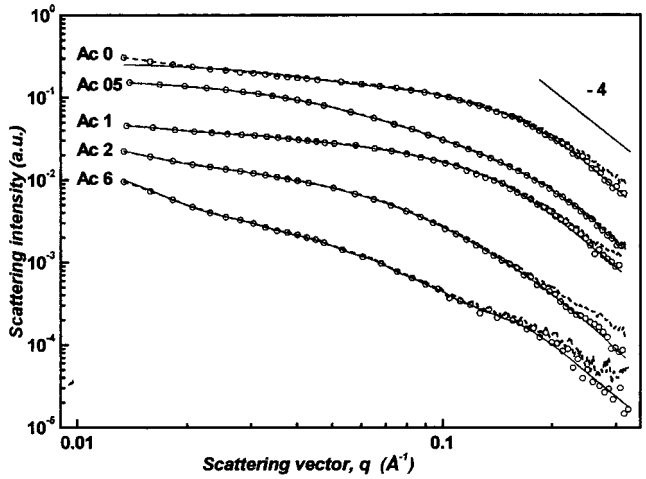

Figure 4. Logarithm of SAXS intensity $I(q)$ (circles) and $I(q)_e$ (dashed lines) as a function of the logarithm of the modulus of the scattering vector q corresponding to colloidal suspensions prepared with different complexing ratio submitted to thermohydrolysis at 70 °C during 65 min. The continuous lines are the fittings of GNOM program to the experimental curves. The straight line with slope −4 at high q represents the theoretical Porod regime (eq 1). The curves corresponding to Ac0, Ac05, Ac1, Ac2, and Ac6 samples were vertically displaced for clarity.

A narrow volume distribution centered at 9.6 Å is observed in Figure 5 for the sol prepared without acetylacetone (Ac0). As the acetylacetone content increases, the maximum of the size distribution decreases and both the width of the distribution and R_{max}, the particle radius corresponding to the volume distribution maximum, increase. As a matter of fact, we have $R_{max} = 9.6$ and 11.5 Å for $c = 0$ and 6, respectively. Moreover, a bimodal size distribution is apparent for $c = 6$. A weak second mode is also observed for $c = 2$.

Figure 6 shows the effect of acetylacetone content on the total number of colloidal particles N and on B, this parameter being proportional to the number of precursor molecules remaining in solution. Increasing the amount of acetylacetone leads to a large decrease in the total number (N) of colloidal particles in the sol. On the contrary, the electron density fluctuation term, B, increases with acetylacetone content, indicating a progressive increase in the concentration of remnant precursor in solution. This feature demonstrates that the addition of acetylacetone hinders the hydrolysis of the precursor, partially preventing condensation.

These results are in agreement with those reported in previous works[8,17,18] concerning the ability of the enolic form of acetylacetone to react with tin alkoxides ($Sn(OR)_4$) and tin halogens (SnX_4, X = F, Cl, Br) to give β-diketone, such as

$$SnX_4 + nH(acac) \rightarrow SnX_{4-n}(acac)_n + HX \qquad (5)$$

The stoichiometric complex prepared with $n = 1$ and $n = 2$ have dimeric and monomeric forms, respectively.[17] The dimeric mono-chelate complex in anhydrous solution is unstable, being rapidly converted into a mixture of tin-containing species followed by slow disproportionation to the monomeric derivative.[17] In the presence of water, this instability of dimeric complex can increase the hydrolysis rate, so increasing the number of the colloidal particles. This proposition is consistent with the maximum value of the number of particles observed for $c = 0.5$ in Figure 6 and with the kinetic behavior shown in Figure 3.

Kinetic[13] and structural NMR[18] studies indicate that, for $c \geq 2$, only monomeric dihalobis(acetylacetonato)tin(IV) complexes are formed and stay in equilibrium with free H(acac) in excess. The rate of intermolecular acetylacetone exchange

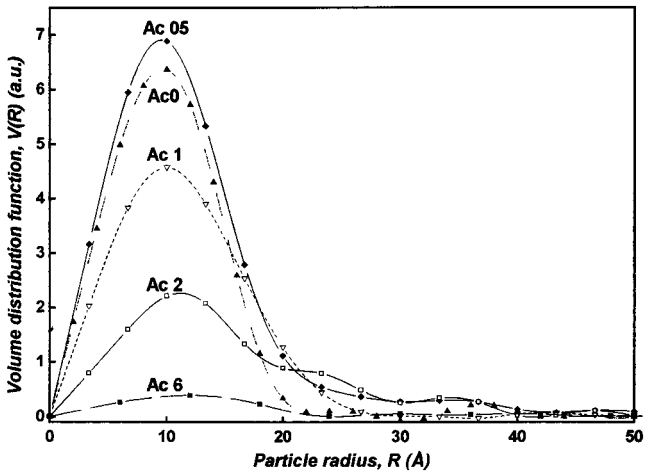

Figure 5. Volume distribution functions of the colloidal particles corresponding to the sols with different complexing ratios, all of them thermohydrolyzed during 65 min at 70 °C.

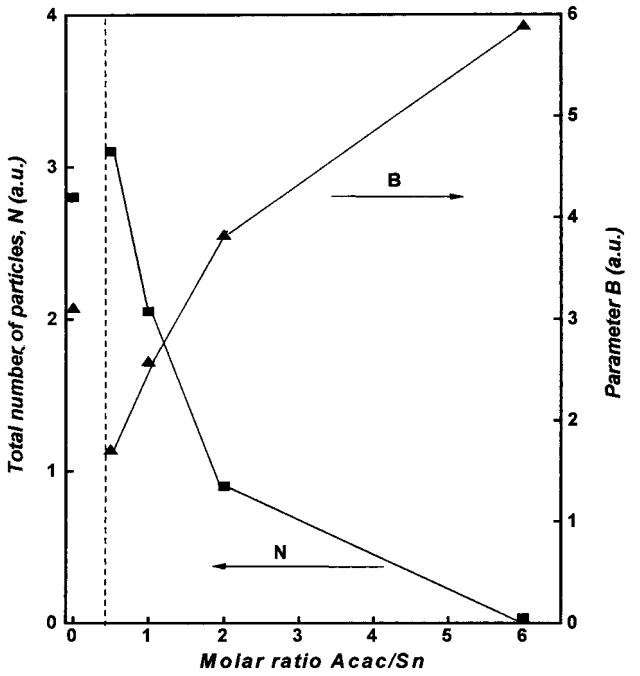

Figure 6. Total number of colloidal particles N and parameter B (proportional to the number of SnO_2-based monomer remnant in solution) as functions of the complexing ratio for isocronous ($t = 65$ min) thermohydrolysis at 70 °C.

between $Sn(acac)_2Cl_2$ and H(acac) is too slow to be measured by NMR but it was estimated to be 100 times smaller than for Cl exchange.[18] The Sn−acac bond is stabilized by the chelate ring and the two parts can remain bonded after hydrolysis,[7,19,20] preventing condensation and the formation of an oxide network. Furthermore, as the chelated tin has 6-fold coordination instead of 4,[8] the reactivity of precursors is lowered. Such low reactivity is supported by light scattering measurements after thermohydrolysis at different temperatures. These analyses demonstrated that colloidal particles are not formed if hydrolysis is performed below 55 °C.

For higher thermohydrolysis temperature, the β-diketonate ligands become more labile and could be released in solution.[11] The SAXS results shown in Figures 5 and 6 indicate that the equilibrium between bonded and free acetylacetone is displaced toward complexation as the complexing ratio increases, leading to a reduction in the number of colloidal particles. Furthermore,

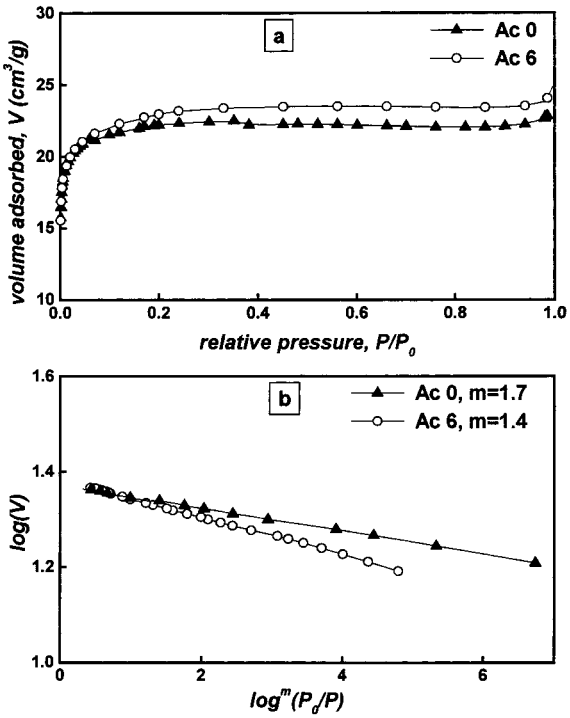

Figure 7. N_2 adsorption isotherms (a) and Dubinin-Astakov plot (b) corresponding to Ac0 and Ac6 freeze-dried powders.

the reduction in the number of growing seeds leads to the increase in polydispersity and average particle size, as expected for the nucleation and growth process.[5] This polydispersity can also be a consequence of the higher ionic strength of the solution, in which a large amount of unreacted precursor favors the aggregation of primary particles.

3.3. Powder Texture. The N_2 adsorption measurements of freeze-dried powders exhibit a type I isotherm shape,[21] typical of microporous solids (Figure 7a). In this case, the properties of the porous texture can be determined by using the Dubinin-Astakhov plot[22] shown in Figure 7b. The linear behavior, observed all over the relative pressure range, indicates that the adsorption isotherms are fully described by the Dubinin-Astakhov relationship:[22]

$$\log V_g = \log V_0 - \beta^m \log^m(P_0/P) \qquad (6)$$

where V_o and V_g represent the total micropore volume and the volume of gas adsorbed at relative pressure (P/P_0), respectively, and β is a parameter related to the average micropore size and adsorbate affinity coefficient. The exponent m assumes values equal to 2 for Gaussian distribution of pore size.

The best fitting by linear regression was determined for all studied samples. The m value decreases from 1.7 to 1.4 when the [acac]/[Sn] ratio increases from 0 to 6. This increasing deviation from the value expected for a Gaussian distribution ($m = 2$) is consistent with the increasing asymmetric broadening of the particle size distribution observed by SAXS for increasing acetylacetone content (Figure 5). Moreover, irrespectively of the complexing ratio, the samples have practically the same total micropore volume, $V_o \cong 0.037 \pm 0.002$ cm^3/g, specific surface area $S_o \cong 200 \pm 10$m^2/g, and average pore size (8.0 ± 0.4 Å). This indicates that the overall texture of the microporous powders is essentially independent of the amount of acetylacetone used as a complexing ligand during the synthesis of SnO_2 colloids.

The observed invariance of the specific interface area suggests the absence of complexed species at the surface of particles.

This hypothesis was confirmed by thermogravimetric analysis carried out on these powders. The thermogravimetric curves corresponding to Ac0 powder and to samples prepared in the presence of acetylacetone practically overlaps. These TGA curves also overlap that corresponding to the powder prepared by alkaline hydrolysis of $SnCl_4$ aqueous solution.[4] Furthermore, no organic groups were observed in the infrared spectra of powder dried at 110 °C. These features indicate the absence of remnant-complexed species after dialysis and freeze-drying processes. Despite the comparable values of particle size in the sol and of average porous size, our results suggest that the particles in freeze-dried powders are not agglomerated. This is in agreement with the observed easy redispersability of these powders either in water or in alcohol.[12]

In short, N_2 adsorption results and those obtained from SAXS measurements of the sols indicate that the average pore size in dried powders is approximately equal to the average size of the colloidal particles in the sols, so that the individual colloidal particles are not strongly affected by aging during dialysis or by the freeze-drying process (i.e., there is not, for example, a growth mechanism leading to larger dense particles). On the other hand, and more important, the results of our N_2 adsorption measurements demonstrate that the micropore volume fraction, specific surface area, and average pore size of powders are independent of the acac content. In addition, results suggest that no acac remains at the surface of the dried particles. SAXS measurements of the sols clearly demonstrated that the increase of acac content strongly affects hydrolysis and polycondensation processes leading to decreasing the number of colloidal particles formed in suspension. The difference in particle size in sols with different acac content is due to an additional weak effect of acac, inducing the partial aggregation of the nanoparticles in sol, but not affecting the final texture of the dried powder. This behavior is remarkably different from that reported for acac-complexed tetravalent metal alkoxides,[7,10] in which the growth of partially condensed species is inhibited by capping with acac ligands and by residual alkoxy groups located at the surface of particles. Thus the growth of these particles is surface controlled and an increase of acac content yields to a decrease of the average particles size. Our results show that this mechanism does not apply in the case of acac-complexed tin chloride precursor, in which the average particle is practically invariant with the [acac]/[Sn] ratio. In this case the growth of primary particles is inhibited by the prompt consumption of the more reactive species, while the stability of suspension toward aggregation is controlled by electrostatic repulsion between the surface charged particles.

4. Conclusion

The hydrolysis and condensation processes of acetylacetone-modified tin tetrachloride precursor can be chemically controlled by varying the complexing ratio ([acac]/[Sn]). The stability of the organic ligands prevents the hydrolysis reactions, reducing the number of colloidal particles formed during thermohydrolysis by a factor 2, when [acac/[Sn] increases from 0 to 2. The excess of acetylacetone ([acac]/[Sn] > 2) in the mother solution favors the aggregation of primary particles, leading to an increase in the average size and size dispersion of the aggregates. The complexed acetylacetone can be released by dialysis resulting in nonagglomerated powders after the freeze-drying process. The porosity, specific surface area, and average pore size of freeze-dried powders are independent of the acac content, so that the mentioned effects of the acac ligand on hydrolysis and condensation processes do not affect significantly the texture of final powders.

Acknowledgment. The financial support provided by LNLS, CAPES/COFECUB, FAPESP, PRONEX (Brazil) is acknowledged.

References and Notes

(1) Santos, L. R. B.; Larbot, A.; Persin, M.; Santilli, C. V.; Pulcinelli, S. H. *J. Sol−Gel Sci. Technol.* **1998**, *13*, 806.
(2) De Souza, A. E.; Monteiro, S. H.; Santilli, C. V.; Pulcinelli, S. H. *J. Mater. Sci.: Mater. Electronics* **1997**, *8*, 267.
(3) Rizzato, A. P.; Santilli, C. V.; Pulcinelli, S. H.; Messaddeq, Y. *J. Non-Cryst. Solids* **1999,** *256&257*, 154.
(4) Santilli, C. V.; Pulcinelli, S. H.; Brito, G. E. S.; Briois, V. *J. Phys. Chem.* **1999**, *B103*, 2660.
(5) Brinker, C. J.; Scherer, G. W. *Sol−Gel Science: The Physics and Chemistry of Sol−Gel Processing*; Academic Press: San Diego, 1990.
(6) Livage, J.; Henry, M.; Sanches, C. *Prog. Solid State Chem.* **1988**, *18*, 259.
(7) Scolan E.; Sanches, C. *Chem. Mater.* **1998**, *10*, 3217.
(8) Gamard, A.; Jousseaume, B.; Toupance, T.; Campet, G. *Inorg. Chem.* **1999**, *38*, 4671.
(9) Gamard, A.; Mabot, O.; Jousseaume, B.; Dascle, M. C.; Toupance, T. Campet, G. *Chem. Mater.* **2000**, *12*, 3419.
(10) Scolan, E.; Magnenet, C.; Masiot, D.; Sanches, C. *J. Mater. Chem.* **1999**, *9*, 2467.
(11) Chatry, M.; Henry, M.; In, M.; Sanches, C.; Livage, J. *J. Sol-Gel Sci. Technol.* **1994**, *1*, 233.
(12) Rizzato, A. P.; Broussous, L.; Santilli, C. V.; Pulcinelli, S. H.; Craievich, A. F. *J. Non-Cryst. Solids.* **2001**, *284*, 61.
(13) Santos, L. R. B.; Santilli, C. V.; Pulcinelli, S. H.; Craievich, A. F. *J. Appl. Cryst.* **2000**, *33*, 605.
(14) Kellermann, G.; Vicentin, F.; Tamura, E.; Rocha, M.; Tolentino, H.; Barbosa, A. F.; Torriani, I.; Craievich, A. F. *J. Appl. Crystallogr.* **1997**, *30*, 880.
(15) Porod, G. *Small Angle X-ray Scattering*; Kratky, O., Glatter O., Eds.; Academic Press: London, 1982; p 17.
(16) Svergun, I.; Semmenyuk, A. V.; Feigin, L. A. *Acta Crystallogr.* **1988**, *A44*, 244.
(17) Chandler, C. D.; Fallon, G. D.; Koplick, A. J.; West, B. O. *Aust. J. Chem.* **1987**, *4*, 1427.
(18) Jones,R. W., Jr.; Fay, R. C. *Inorg. Chem.* **1973**, *12*, 2599.
(19) Kenppler, B. K.; Friesen, C.; Vongerichten, H. G.; Vogel, E. *Structure Bonding* **1991**, *78*, 97.
(20) Hoebbel, D.; Reinert, T.; Schimidt, H.; Arpac, E. *J. Sol-Gel Sci. Technol.* **1997**, *10*, 115.
(21) Gregg, S. J.; Sing, K. S. W. *Adsorption, Surface Area and Porosity*; Academic Press: London, 1982; Chapter 6.
(22) Dubinin, M. M.; Astakhov, V. A. *Izv. Akad. Nauk. SSSR Ser. Khim.* **1971**, *1971*, 5.